

2022

Minimum Rim Width and Lamina Cribrosa Depth in Non-Glaucomatous and Glaucomatous U.S. Veterans

Jacob Hillard OD

Department of Veterans Affairs, jakehillard.o.d@gmail.com

Rachel Druckenbrod OD

Department of Veterans Affairs, rachel.druckenbrod@va.gov

Baharak Asefzadeh OD

Department of Veterans Affairs, bostonbaha@yahoo.com

Follow this and additional works at: https://athenaeum.uiw.edu/optometric_clinical_practice



Part of the [Education Commons](#), [Optometry Commons](#), and the [Other Medicine and Health Sciences Commons](#)

The Athenaeum provides a publication platform for fully open access journals, which means that all articles are available on the Internet to all users immediately upon publication. However, the opinions and sentiments expressed by the authors of articles published in our journal does not necessarily indicate the endorsement or reflect the views of the University of the Incarnate Word and its employees. The authors are solely responsible for the content of their work. Please address questions to athenaeum@uiwtx.edu.

Recommended Citation

Hillard J, Druckenbrod R, Asefzadeh B. Minimum Rim Width and Lamina Cribrosa Depth in Non-Glaucomatous and Glaucomatous U.S. Veterans. *Optometric Clinical Practice*. 2022; 4(2):27. doi: 10.37685/uiwlibraries.2575-7717.4.2.1036. <https://doi.org/10.37685/uiwlibraries.2575-7717.4.2.1036>

This Article is brought to you for free and open access by The Athenaeum. It has been accepted for inclusion in *Optometric Clinical Practice* by an authorized editor of The Athenaeum. For more information, please contact athenaeum@uiwtx.edu.

Minimum Rim Width and Lamina Cribrosa Depth in Non-Glaucomatous and Glaucomatous U.S. Veterans

Abstract

Purpose: Assess the utility of the MRW and lamina cribrosa depth measurements for detecting differences between non-glaucomatous and glaucomatous U.S. Veterans. Compare inter-eye differences of individuals with glaucoma.

Method: 38 subjects were recruited per group: Group 1 included one eye of non-glaucomatous participants, and Group 2 included each qualifying eye of participants with glaucoma. Analysis compared Group 1 with the more affected eye only of Group 2 participants, and separately between the more and less affected eyes of group 2 participants. MRW measurements were obtained with Heidelberg Eye Explorer® (HEYEX). Average lamina cribrosa depths were measured manually utilizing HEYEX.

Results: 26 subjects from Group 1 and 33 subjects from Group 2 were included. A significantly thinner MRW was found in glaucomatous eyes vs. non-glaucomatous eyes (210 μm vs. 309 μm ; $P < .001$). The normative database in HEYEX had an 85% sensitivity and 92% specificity to detect glaucomatous nerves. Among the 27 participants in Group 2 who had both eyes tested, eyes with more advanced visual field loss showed significantly thinner global MRW compared to fellow eyes (203 μm vs. 224 μm $P = .03$). Lamina cribrosa depths were non-significantly deeper in glaucomatous vs. non-glaucomatous eyes (476 μm vs. 429 μm $P = .17$).

Conclusions: The MRW parameter differentiates between glaucomatous and non-glaucomatous optic nerves. Lamina cribrosa depths were non-significantly deeper in glaucomatous vs. non-glaucomatous participants. Post-hoc inter-eye data analysis suggested that inter-eye differences in gMRW values of glaucomatous eyes reflect asymmetric damage as correlated with the visual field

Keywords

Glaucoma, Minimum Rim Width, Lamina Cribrosa Depth, Optic Nerve Head

Creative Commons License



This work is licensed under a [Creative Commons Attribution-NonCommercial-Share Alike 4.0 International License](https://creativecommons.org/licenses/by-nc-sa/4.0/).

Cover Page Footnote

Acknowledgements The authors would like to thank Angela Turalba, M.D and Claude Burgoyne, M.D for their advice in the conception and design of this study.

INTRODUCTION

Although the relationship between glaucoma and elevated intraocular pressure is well-established, the exact pathophysiology of glaucoma remains unclear. An elevated intraocular pressure measurement alone is not sufficient to predict if a particular patient has glaucomatous optic nerve damage or if they will develop it, so additional mechanisms must contribute. Current theories implicate a mechanical mechanism of stress and strain within optic nerve head tissues as a cause for glaucomatous retinal ganglion cell damage.^{1,2} These environmental disturbances are influenced by the balance of intraocular pressure and tissue properties.^{3,4} When strain within the nerve reaches a certain point, compression and loss of the retinal nerve fiber layer (RNFL) occurs. This results in thinning of the neuro-retinal rim which is characteristic of glaucomatous optic neuropathy. Rim thinning is historically assessed clinically with ophthalmoscopy and estimated by determination of the “cup-to-disc ratio” (C/D ratio). It is well known that the C/D ratio is an unreliable measure with high inter-examiner variability.^{5,6} A more precise and accurate measure of the neuro-retinal rim is required to improve clinical analysis of the glaucomatous optic nerve head.

A new, highly reproducible⁷⁻⁹ objective parameter to detect glaucoma and its progression has recently been described. Named “Bruch’s-membrane-opening-minimum-rim width” (MRW), it is an optical coherence tomography (OCT) measurement of the minimum tissue thickness at the perimeter of the optic disc between the internal limiting membrane and the termination of Bruch’s membrane.¹⁰ The termination of Bruch’s membrane around the circumference of the optic nerve is termed Bruch’s Membrane Opening (BMO) and it creates a tissue plane largely perpendicular to the examiner point of view when looking through the pupil. MRW is not required to be measured along the plane of BMO and is more often at an angle to BMO. By measuring the tissue thickness (MRW) at the BMO circumference, pathological changes to the structure of the optic nerve and surrounding tissues can also be indirectly captured. These pathological changes are thought by many to be a change more unique to glaucomatous neuropathy than ganglion cell loss.¹¹ MRW is calculated semi-automatically using OCT software (HEYEX, Heidelberg Engineering Inc, Franklin, MA) at 48 points along the circumference of BMO. MRW has performed as well,¹² or slightly better than, other OCT measures for glaucoma detection. In experimental glaucoma in non-human primates, manually-delineated MRW detected the onset of glaucoma more frequently than traditional peripapillary retinal nerve fiber layer thickness (pRNFLT) measurements.¹³ In a human study, the sensitivity of MRW to detect glaucomatous vs. non-glaucomatous eyes at 95% specificity was greater than pRNFLT.⁶

Improvements in OCT have enabled in-vivo visualization of deeper optic nerve tissues, including the morphology of the lamina cribrosa (hereafter “lamina”), previously only measurable after enucleation.¹⁴ Anterior lamina cribrosa depth (ALCD), or the axial distance between the BMO plane and the anterior surface of the lamina, increases as the lamina is displaced posteriorly in early glaucoma.^{15,16} After therapeutic lowering of intraocular pressure, the lamina moves anteriorly in subjects with primary open angle glaucoma¹⁷⁻²² and ocular hypertension.¹⁷ This post-treatment morphological change has been linked with relative stabilization of pRNFLT over time.²² Reduction of ALCD from anterior movement of lamina after IOP-lowering has been shown to vary by factors such as disc size,²³ age,¹⁸ corneal properties,¹⁷ and race.²⁴

Early detection of glaucoma in clinical practice is desirable, and the goal of treatment is to minimize pathological changes to the optic nerve. OCT-derived measurements such as MRW and ALCD may provide an avenue for improved detection of glaucomatous damage or propensity for development of glaucoma. Further characterization of normal and diseased optic nerve morphology with advanced imaging techniques that are simple to use clinically is necessary to achieve this goal. This study aimed to analyze differences in MRW and ALCD between glaucomatous and non-glaucomatous eyes, as well as to compare MRW and ALCD measurements between more-affected and less-affected eyes of glaucoma participants, with the hypothesis that glaucoma is associated with significantly thinner MRW and with deeper ALCD.

METHODS

This cross-sectional study was approved by the Institutional Review Board of VA Boston Healthcare System. The study adhered to the tenets of the Declaration of Helsinki. Written informed consent and authorization for use of individually identifiable health information were obtained from all participants after explaining the study and the risks associated before participation. This material is the result of work supported with resources and the use of facilities at the Jamaica Plain Veterans Affairs Hospital in Boston, MA. The contents of this publication do not represent the views of the U.S. Department of Veterans Affairs or the United States Government.

STUDY PARTICIPANTS

U.S Veterans between the ages of 18 and 89, enrolled in the VA Boston Healthcare system and receiving eye examinations, were screened by chart review for study eligibility. Group 1 consisted of non-glaucomatous participants (mean age: 63.0, 88.5% male), and Group 2 consisted of glaucomatous participants (mean age 73.8, 100% male). Clinical diagnosis of glaucoma was determined using dilated assessment of the optic nerve head by an experienced optometrist or ophthalmologist, automated visual field testing with the Humphrey Field Analyzer II (Carl-Zeiss Meditec, Dublin, Ca), and Spectralis OCT (Heidelberg Engineering GmbH, Heidelberg, Germany) analysis of the optic nerve retinal fiber layer and macular thicknesses (clinicians did not have access to MRW analysis for diagnosis). The following were required for participation: available records from an eye examination within the past 12 months, Snellen visual acuity of at least 20/40, refractive error less than six diopters of sphere and no more than two diopters of cylinder, absence of previous refractive or intraocular surgery besides uncomplicated cataract or glaucoma surgeries, absence of pathology (other than glaucoma) that would complicate OCT imaging or affect optic nerve function. Specifically excluded conditions were: diabetic retinopathy exceeding “moderate non-proliferative” per the international clinical diabetic retinopathy severity scale,²⁵ macular edema, advanced age-related macular degeneration as defined by the Age-Related Eye Disease Study (AREDS),²⁶ history of retinal vessel occlusion, significant retinal scarring, and significant epiretinal membrane. Additional exclusion criterion for Group 1 included: suspicion of glaucoma (based on elevated intraocular pressure and/or suspicious optic nerve appearance by clinical exam or OCT imaging), history of ocular hypertension in either eye, abnormal visual fields (VF) (defined as reliable fields with a pattern deviation map containing three contiguous non-edge points significantly different from age-matched norms at a $P < 0.05$ level, at least one of which was significant at the $P < .01$ level), or a glaucoma hemifield test reported as “outside normal limits.”

One eye of each participant in Group 1 was selected to be tested. If both eyes of a Group 1 participant qualified, the eye with the better visual acuity or lower refractive error was selected. If both eyes of a participant in Group 2 qualified for the study, both eyes were tested and only the more-affected eye (defined as the eye with the higher pattern standard deviation (PSD) on the VF) was used in comparison with Group 1.

DATA COLLECTION

VISUAL FIELDS

Automated perimetry with the Humphrey VF 24-2 protocol (HFA II; Carl Zeiss Meditec, Inc, Dublin, CA) was performed for all participants who did not have a reliable VF test from the last 12 months. Reliability was acceptable if false positives and negatives were both $\leq 20\%$ and fixation losses were $\leq 33\%$. If the perimetrist's notes and gaze tracking were acceptable, then fixation was considered acceptable. If a VF was not reliable, it was repeated once before the participant was excluded.

AUTOMATED KERATOMETRY

Corneal curvature was obtained on all tested eyes by automated keratometry (KR8800, Topcon Corporation, Singapore). This was entered into the OCT prior to scanning to allow for adjustment by the OCT software for eye specific magnification. Incorrect values were erroneously entered for nine participants, theoretically affecting the accuracy of measurements along the retinal plane such as BMO area; therefore, the affected data were not used when comparing to the normative database. The maximum error on MRW measurement was less than 0.15% in any group, and this was considered negligible.

OPTICAL COHERENCE TOMOGRAPHY

After inputting participant information and aligning the imaging system, the infrared fundus image was focused using the instrument focus knob. Semi-automatic detection of the participant's fovea and the center of the optic disc was performed, and the angle between the fovea-to-Bruch's membrane (FoBMO) axis and the horizontal axis of the instrument was automatically calculated. All further scans were automatically centered on the optic disc and respected the FoBMO axis. Eye tracking was engaged, and 24 radial B-scans and three circular B-scans were obtained. Twenty-five to 100 individual scans were averaged to create each B-scan (a pre-programmed setting of the instrument, where the number of scans depends on the type of scan obtained). If scan quality was unacceptable (due to unacceptable qualitative contrast between layers, or where the averaged quality value was < 16), one repeat scan was attempted. Participants for whom quality scans were not possible were excluded from the study.

FUNDUS PHOTOGRAPHY

Color fundus photography (CR-2 Plus, Canon U.S.A, Melville, NY) was obtained in the studied eye(s).

IMAGE ANALYSIS

After acquiring OCT scans, the MRW and pRNFLT were automatically calculated by the software (GMPE software, Heidelberg) and similarly compared to the Heidelberg normative database. For MRW calculation, since 24 radial B-scans were automatically acquired through the center of the disc, this allowed for MRW measurements at 48 locations (2 locations for each scan). At each such location, a measurement between the edge of Bruch's membrane (confirmed at the time of image acquisition) and the point of the automatically segmented internal limiting membrane with the closest proximity was calculated. The pRNFLT was calculated along the circular B-scans. Comparisons to the normative database were given as an overall average, or "global" value (global MRW or gMRW), and by optic disc sector including superior temporal (ST), superior nasal (SN), nasal (N), inferior nasal (IN), inferior temporal (IT) and temporal (T). Tissue thickness was reported as an absolute measurement and as a percentile of the normative data. All B-scans were individually inspected for segmentation accuracy and manually corrected where required.

ALCD MEASUREMENTS

B-scans were displayed with square pixels and ALCD measurements were made within HEYEX. Brightness and contrast of the images were adjusted within the manufacturer's software for optimal visualization of structures. Respecting the FoBMO axis, vertical (B-scan #1/24; Figure 1A) and horizontal (B-scan #13/24; Figure 1C) scans were reviewed to verify visibility of the edge of Bruch's membrane and the anterior surface of the lamina. If poor image contrast did not allow for complete visualization of structures, the scans nearest the horizontal and vertical axes were assessed (within 7.5 degrees of the superior/inferior or temporal/nasal axis).

In the vertical B-scan, the maximum depths of the anterior surface of the superior and inferior halves of the lamina from the Bruch's membrane opening (BMO) plane were identified and a manual measurement was acquired perpendicular to the BMO plane (Figure 1B and 1D). Since the lamina contour is "W" shaped along the vertical axis, creating locations of maximal depth on either side of the center, two measurements of ALCD were taken in the vertical plane (Figure 1B). Since

shadowing from blood vessels prevents reliable viewing of the lamina nasally, ALCD measurement was taken at the point of maximum lamina depth only on the temporal half of the optic nerve head scan (usually occurring near the center of the disc; Figure 1D). An average of the three ALCD measurements was calculated and represented a single participant's averaged maximum ALCD (aALCD). The eye was not included in aALCD analysis if it was not possible to reliably make all three measurements.

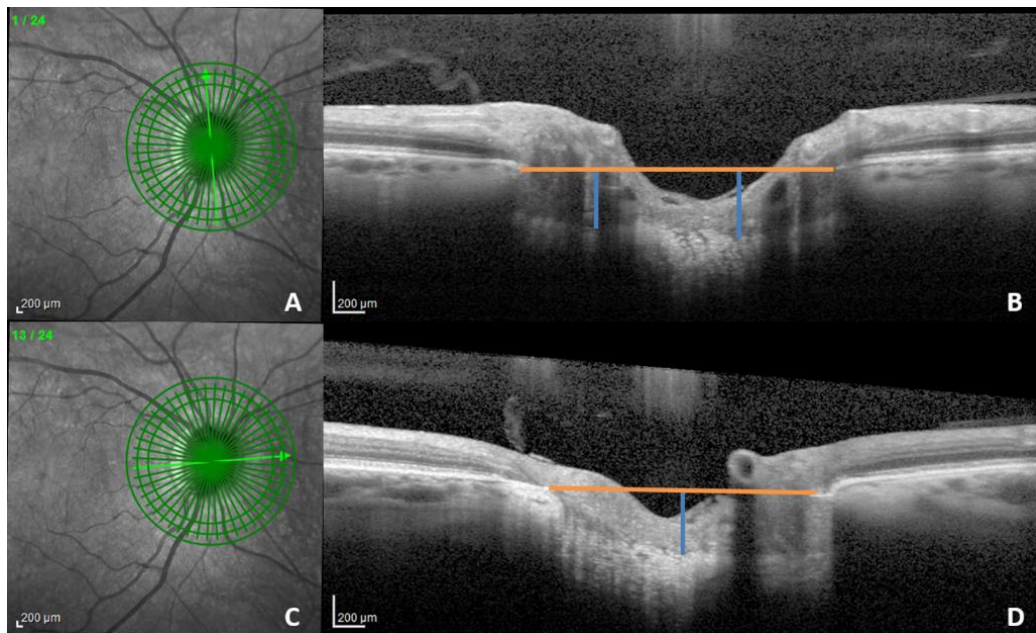


Figure 1: A and C: Scanning laser ophthalmoscope images of the optic nerve with green lines indicating the locations of the captured scans. The bright green arrow indicates the location and orientation of the OCT B-scan to the right. B and D: The orange line is an example of the line placed between the BMO edges on either side of the nerve, and the blue lines show where the ALCD measurements were taken in the superior and inferior half of the nerve (top) and temporal half of the nerve (bottom) with respect to the FoBMO axis.

STATISTICAL ANALYSIS

To achieve 95% statistical power allowing for 30% participant exclusion, 38 participants per group (76 total) were recruited. The primary dependent variables were MRW values (global and sectoral). The secondary dependent variables were pRNFLT (global or gRNFL), VF pattern deviation, and aALCD. Possible confounding variables were age, refractive error, gender, race, and BMO area. Gender and race were not considered as covariates in this study due to the low

number of female ($n = 3$) and non-Caucasian ($n = 20$) subjects. Statistical significance was considered at $P < .05$. When comparing Groups 1 and 2, only the more-affected Group 2 eye was used (hereafter called the “test” eye).

Pearson correlation was used to identify confounding variables, and analysis of covariance (ANCOVA) tests were used to detect differences in means between groups while adjusting for covariates. The assumption of homogeneity of variance was tested by Levene’s statistic. A Student’s t-test was used unless Levene’s test was significant, in which case a Welch’s t-test was used. A general linear model pairwise comparison was performed when comparing the test and fellow eyes of Group 2 participants. All planned statistical calculations were performed using SPSS (IBM Corp. Released 2017. IBM SPSS Statistics for Windows, Version 25.0. Armonk, NY: IBM Corp).

Sensitivity and specificity of the Heidelberg normative database were calculated to differentiate glaucomatous vs. non-glaucomatous eyes. Sensitivity was calculated by using the number of true positives (more-affected group 2 eyes with at least 1 sector reported as “borderline” or “outside normal limits”) divided by the sum of true positives and false negatives (more affected group 2 eyes with all sectors reported as “within normal limits”). Specificity was calculated by taking the number of true negatives (normal eyes with all sectors considered “within normal limits”) divided by the sum of the number of true negatives and false positives (normal eyes with at least one sector reported as “borderline” or “outside normal limits”).

RESULTS

DEMOGRAPHICS

Thirty-eight participants were recruited for each group. After exclusion, 26 participants from Group 1 and 33 participants from Group 2 remained. The most common reasons for exclusion were unreliable VF testing or poor-quality OCT images. Both eyes were included for 27 participants in Group 2. Age was significantly different between Groups 1 and 2 ($P < .001$). Demographics and secondary dependent variables are given in Table 1 (comparison between Groups 1 and only the test eye of Group 2 participants), and Table 2 (comparing test and fellow eyes of bilaterally tested Group 2 participants). For comparison, Figure 2 displays the visual field Mean Deviation (rather than VF PSD) of each group. Of note, there are 2 Group 1 eyes that are outliers which were not excluded from the study as the pattern deviation map and glaucoma hemifield did not meet protocol exclusion criterion. A manual review of the data from these subjects revealed they

had a VF PSD of 1.5 dB and 1.9 dB. They did not have MRW with global or sector values considered outside the 95% confidence interval of the instrument's normative database. Among all included glaucomatous participants, 18 out of 33 participants had visual field testing from a different day than the OCT imaging. The average elapsed time between visual field testing and OCT imaging was 3 months.

GROUP 1 VS. GROUP 2 ANALYSES

Unless otherwise written, results are given as (mean, 95% CI). The gMRW for Group 1 and Group 2 was (328 μ m, standard deviation: 52 μ m) and (195 μ m, standard deviation: 52 μ m). There were significant between-group differences in BMO area ($P < .001$), VF PSD ($P < .001$), and gRNFL (correcting for BMO and age; $P < .001$). When testing all Group 1 eyes and more-affected eyes of Group 2 participants, BMO area ($P < .001$, $r = -0.54$) and age ($P < .001$, $r = -0.48$) were significantly correlated with gMRW. Correcting for differences in BMO area and age, gMRW was significantly thinner in Group 2 (210 μ m, 190 – 230 μ m) vs. Group 1 (309 μ m, 286 – 333 μ m). Table 3 lists global and sectoral MRW values for Groups 1 and 2. MRW sector and group significantly interacted ($P < .001$, eta squared 0.34), but no interaction between other factors was found. MRW was significantly different comparing respective sectors of each group (all $P < .001$).

Including those with the correct C-curve entered into the imaging device before imaging, the numbers and percentages of normal and glaucomatous participants who had global or sector MRW outside the Heidelberg Spectralis® normative database 95% confidence interval are shown in Figure 3. In Group 1, 8.3% of eyes and 85.1% of more-affected Group 2 eyes in this analysis had at least one sector reported as outside of the 95% confidence interval, which resulted in a sensitivity of 85.1% and a specificity of 91.7%.

| GRP | "N" | Age | % Ca | % AA | % Male | Sph. equivalent | IOP | FoBMO angle | BMO Area | G RNFL | VF PSD |
|-----|-----|-----------------|------|------|--------|-----------------|---------------|-------------|-----------------|--------------|---------------|
| 1 | 26 | 63.0 (12.2)* | 80.8 | 15.4 | 88.5 | 0.53 (1.8) | 15.8 (2.6) | -7.2 (4.4) | 1.66 (0.30)* | 93.7 (7.9)† | 1.5 (0.2)* |
| 2 | 33 | 73.8 (9.4)* | 54.5 | 33.3 | 100 | 0.13 (1.6) | 14.5 (4.6) | -7.3 (3.9) | 2.11 (0.46)* | 68.8 (13.9)† | 5.4 (3.0)* |

Table 1: Group (GRP) demographics. Group 1 (non-glaucomatous) and Group 2 (test eye of glaucomatous participants). The number of participants (N), percentages of participants self-identifying as Caucasian (Ca) and African American (AA) are given. Averages of spherical equivalent (Sph. equivalent), intraocular pressure (IOP), fovea-to-Bruch's membrane opening angle (FoBMO angle), Bruch's membrane opening area (BMO Area), global retinal nerve fiber layer measurement (gRNFL), and visual field pattern standard deviation of the visual field test (VF PSD) are also given. Mean shown with the standard deviation in parenthesis. * Is $p < 0.001$

† Is $p < 0.001$ adjusted for age, BMO

| GRP | "N" | Age | % Ca | % AA | % Male | Spherical Equivalent | IOP | FoBMO angle | BMO Area | G RNFL | VF PSD |
|----------------|-----|----------------|------|------|--------|----------------------|---------------|-------------|----------------|-----------------|---------------|
| 2a "test" | 27 | 73.2 (10.0) | 51.9 | 33.3 | 100 | 0.25 (1.8) | 14.6 (4.5) | -7.1 (4.2) | 2.10 (0.48) | 70.6 (13.7)* | 5.0 (2.9)* |
| 2b "fellow" | | | | | | 0.43 (1.7) | 14.5 (3.5) | -7.2 (3.2) | 2.06 (0.43) | 79.4 (12.0)* | 2.2 (1.0)* |

Table 2: Group 2 test eye vs. fellow eye demographics. Group 2a includes the test eye (higher “visual field pattern standard deviation” or VF PSD) of Group 2 participants who had both eyes tested and meeting analysis criterion. Group 2b includes the fellow eye of Group 2 participants (lower VF PSD) with both eyes meeting analysis criterion. The number of participants (N), percentages of participants self-identifying as Caucasian (Ca) and African American (AA) are given. Averages of spherical equivalent (Sph. equivalent), intraocular pressure (IOP), fovea-to-Bruch’s membrane opening angle (FoBMO angle), Bruch’s membrane opening area (BMO Area), global retinal nerve fiber layer measurement (gRNFL), and VF PSD are also given. Mean shown with the standard deviation in parenthesis. The “N”, age, gender, and races were the same in 2a and 2b. Spherical equivalent, IOP, FoBMO angle, and BMO area were not statistically different between groups 2a and 2b (all $p>0.4$).

* $p<0.01$ pairwise comparison test vs. fellow eyes

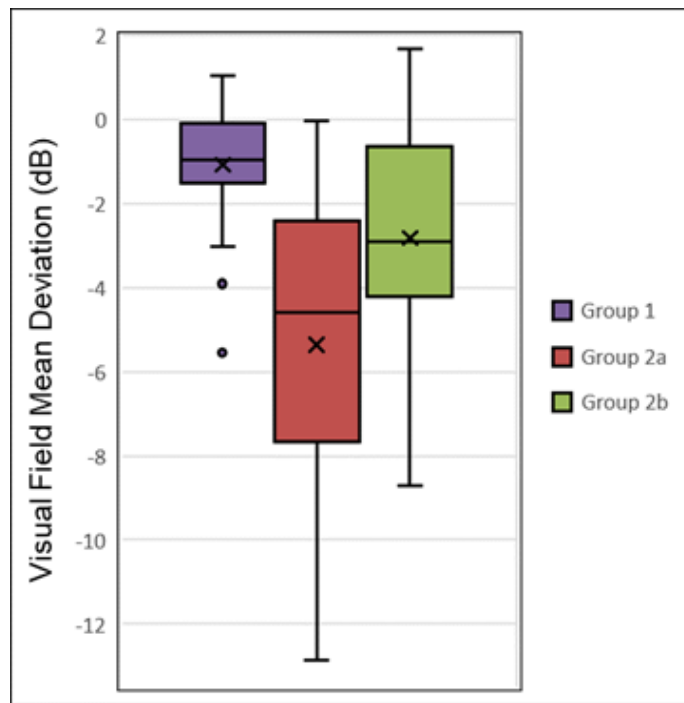


Figure 2: Box and whisker plots of the median (solid black line), mean (“x”), quartile ranges, and outliers (circles) of the visual field mean deviation values for Group 1 participants, Group 2 “test” eyes (Group 2a), and the Group 2 “fellow” eyes (Group 2b).

| Group | Global | Superior-Temporal | Temporal | Inferior-Temporal | Inferior-Nasal | Nasal | Superior-Nasal |
|-------|-----------------|-------------------|-----------------|-------------------|-----------------|-----------------|-----------------|
| 1 | 328.4 (52.2) | 306.7 (68.4) | 230.1 (48.4) | 347.5 (69.8) | 404.3 (67.8) | 367.9 (58.5) | 367.9 (80.5) |
| 2 | 194.8 (51.6) | 156.5 (57.7) | 138.4 (39.9) | 188.1 (66.4) | 239.8 (76.7) | 237.4 (76.5) | 204.8 (61.9) |

Table 3: Group 1 vs. Group 2 minimum rim width (MRW) values given in microns with the standard deviation in parentheses. Using an ANCOVA correcting for age, and BMO area, global values were statistically significant between groups ($p < 0.001$). All sectors were statistically different between groups. A multivariate general linear model including age and BMO area confirmed an effect of age and BMO area ($p < 0.05$) on MRW values and a significant difference between each group for each sector

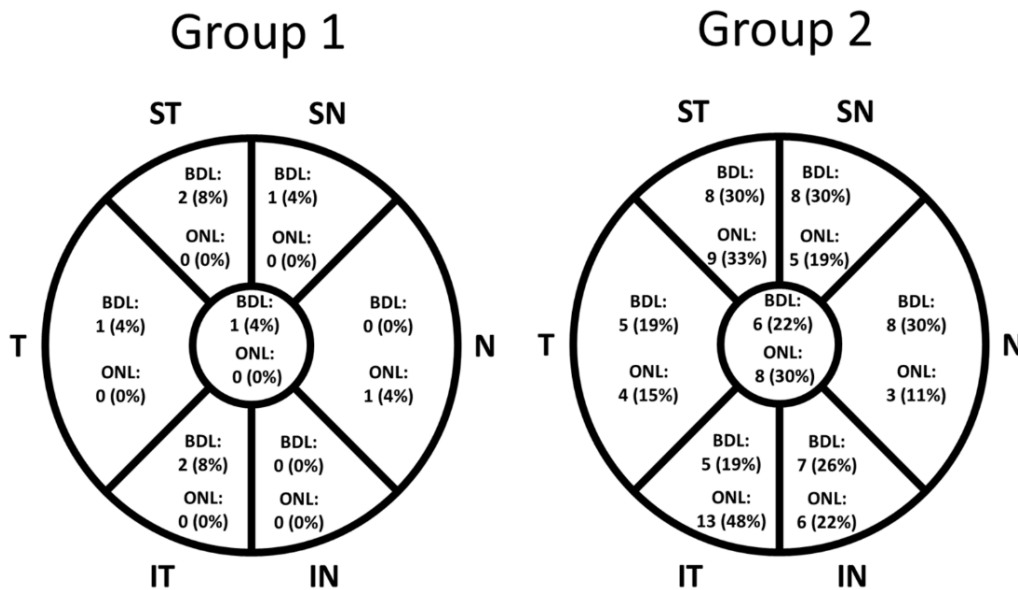


Figure 3: Sectoral analysis showing the number and (percent) of Group 1 and 2 participants with “borderline” (BDL) or “outside normal limits” (ONL) on their minimum rim width analysis. Twenty four participants from Group 1 and 27 participants in Group 2 for whom the corneal curvature was corrected were included. ST = superior temporal, T = temporal, IT = inferior temporal, IN = inferior nasal, N = nasal, SN = superior nasal. Center circle = global

The aALCD was (429 μm , 384 – 474 μm) in Group 1 and (476 μm , 427 – 526 μm) in Group 2 ($P = .17$). There was no correlation of aALCD with age ($P = .50$) or BMO area ($P = .29$) when including all Group 1 eyes and the test eyes of Group 2 participants. Given previous reports correlating age with ALCD and disc size with ALCD, an ANCOVA was performed for the difference between aALCD controlling for age and BMO area in Group 1 (416 μm , 353 – 479 μm) versus Group 2 (485 μm , 435 – 535 μm) without statistical significance ($P = .11$, observed power 0.36).

GROUP 2 INTER-EYE PAIRED ANALYSIS

The mean gMRW of the test (more affected) eye (203 μm , standard deviation 54 μm) was significantly smaller than in the fellow (less affected) eye (224 μm , standard deviation 54 μm) (mean difference: -21 μm , -39 to -3 μm) ($P = .03$). Additional analysis correcting for BMO size did not change this result (data not shown). A sectoral analysis correcting for BMO size showed a significantly lower MRW in the test eye as compared to the fellow eye for each sector except superior temporal (mean difference -15 μm , -27 to 1 μm) ($P = .06$) and nasal ($P = .24$) sectors. These results did not change when correcting for BMO size (data not shown). Group 2 test eyes had thinner gRNFL (mean difference: -8 μm , -15 to -3 μm) ($P = .004$) and significantly larger VF PSD than fellow eyes (5.0 dB, 3.9 – 6.1 dB vs. 2.2 dB, 1.8 – 2.6 dB) ($P < .001$).

Test eyes had non-significantly deeper aALCD (464 μm , 410 – 518 μm) compared to fellow eyes (459 μm , 411 – 507 μm) ($P = .73$). No significant correlation between the BMO area and aALCD was found ($P = .41$). A post-hoc analysis was performed in which inter-eye aALCD, gMRW, gRNFL, PSD, and BMO area differences were calculated by subtracting the respective values of the fellow eye from the test eye (ΔaALCD , ΔgMRW , ΔPSD , and ΔBMOA respectively) (Figure 4 a-d). ΔgRNFL was also calculated but is not displayed in Figure 4. Correlations between these delta values were then explored. A negative correlation between ΔgMRW and ΔaALCD (Figure 5a, $r = -0.47$ $P = .01$) and between ΔgMRW and ΔPSD (Figure 5b, $r = -0.46$ $P = .02$) was detected. ΔgRNFL and ΔPSD were also negatively correlated (Figure 5c, $r = -0.46$ $P = .02$), however, ΔgRNFL and ΔaALCD were not ($P = .10$) (data not shown). No correlation was found between ΔPSD and ΔaALCD ($P = .46$) (data not shown).

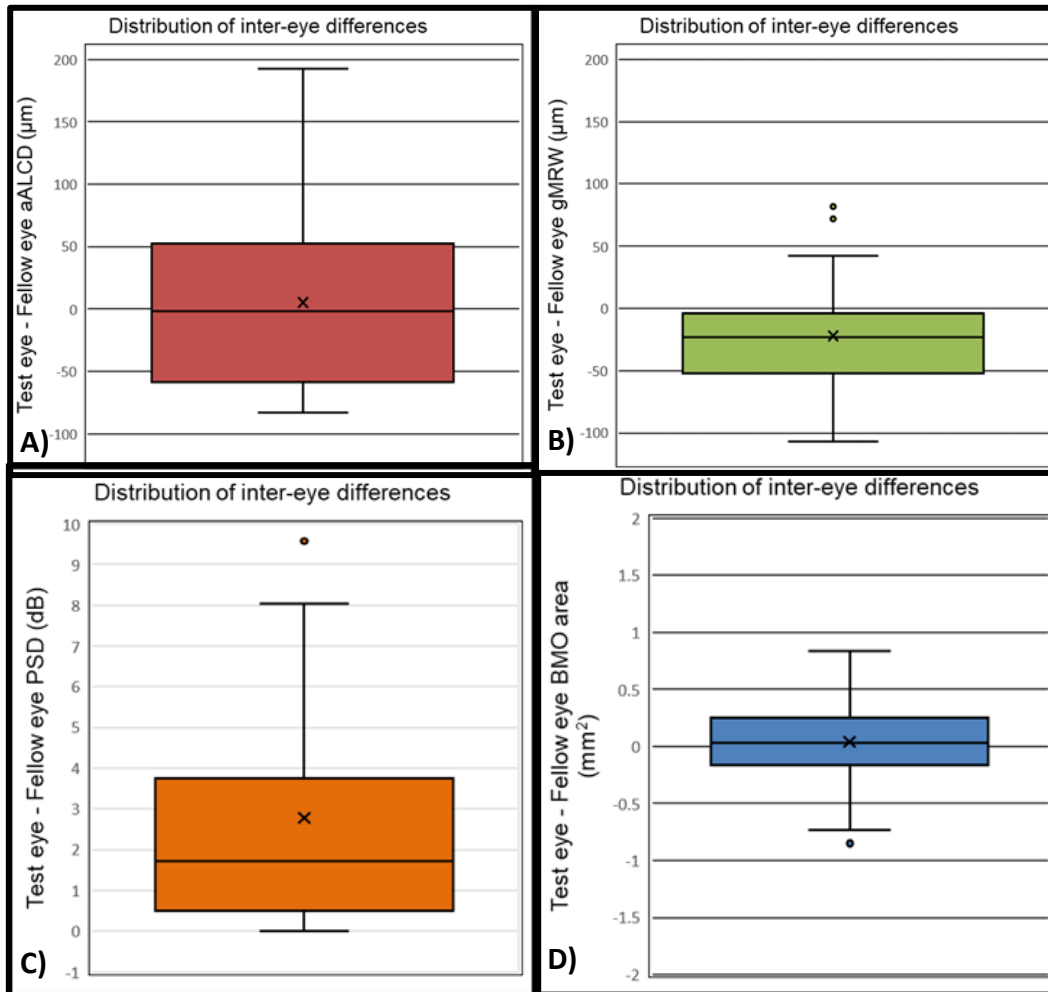


Figure 4: For each participant in Group 2, the average anterior lamina cribrosa depth (aALCD), global minimum rim width (gMRW), Bruch’s membrane opening area (BMO), visual field pattern standard deviation (PSD) average values from the fellow eye were subtracted from their respective parameter value in the test eye. Displayed above are box and whisker plots of the median (solid black line), mean (“x”), quartile ranges, and outliers (circles). The differences are listed on the left vertical axis of each respective plot. A) Displays the difference in ALCD (red) B) displays the difference in gMRW (green), C) Displays the difference in visual field pattern standard deviation (orange), D) Displays the difference in BMO area (blue).

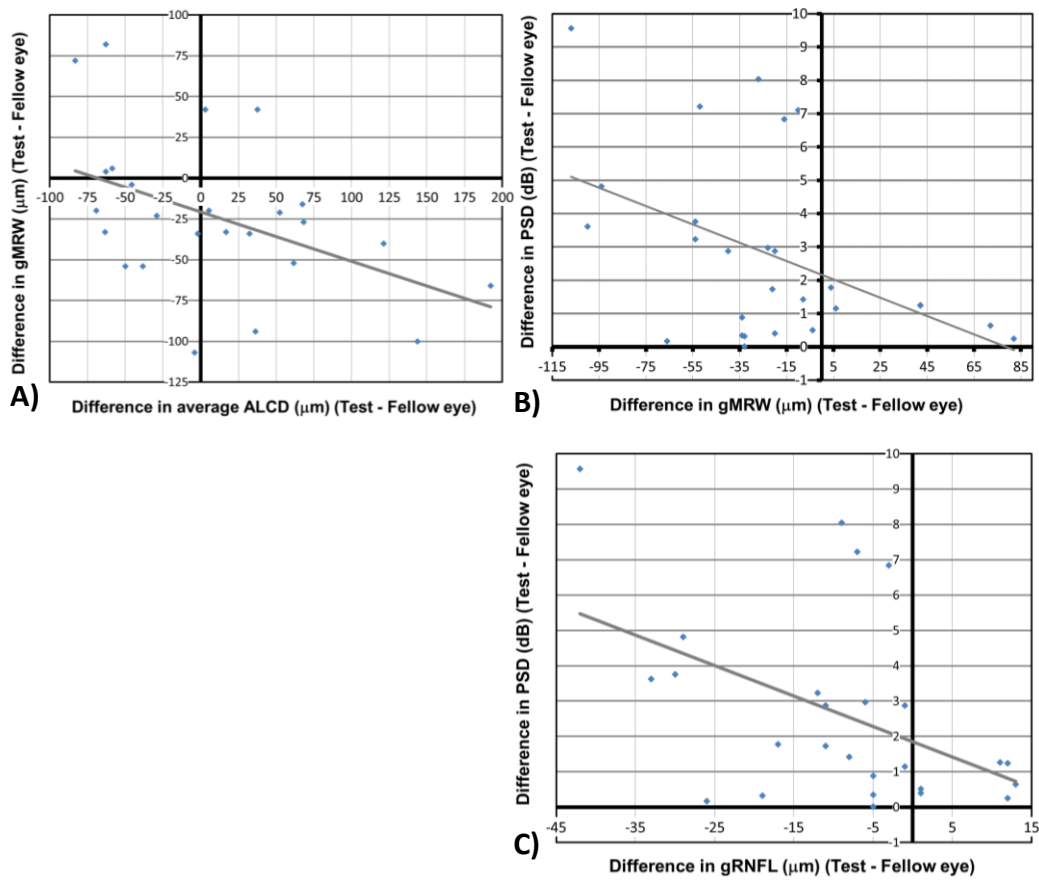


Figure 5: All difference values in the comparisons in this figure are obtained by subtracting the fellow eye's value from the test eye's value. A) Graph of the differences in global minimum rim width (gMRW) vs. the differences in average anterior lamina cribrosa depth (aALCD). Pearson's correlation value is $r = -0.47$, $p = 0.01$. B) Graph of the differences in visual field pattern standard deviation (PSD) vs. the differences in gMRW. Pearson's correlation value is $r = -0.46$, $p = 0.02$. C) Graph of the differences in PSD vs. the differences in global retinal nerve fiber layer (gRNFL). Pearson's correlation value is $r = -0.46$, $p = 0.02$. The difference in gRNFL and difference in aALCD were not correlated ($P = .10$) nor were the difference in PSD and difference in aALCD ($P = .46$). (Data not shown).

DISCUSSION

MINIMUM RIM WIDTH

GROUP 1 VS. GROUP 2 ANALYSES

Correcting for differences in age and BMO area, MRW was significantly thinner in glaucomatous vs. control eyes both when using the “global” average of the MRW thickness and when comparing respective sectors of the rim. Chauhan et al.⁶ described 107 participants with open-angle glaucoma and 48 healthy controls with median gMRW of 182.7 μ m (interquartile range (IQ) 142.2 - 217.7 μ m) and 316.5 μ m (IQ 275.4 - 361.7 μ m) respectively. These values are similar to the present study where gMRW (mean \pm standard deviation) of the glaucoma group and control group were 195 \pm 52 μ m and 328 \pm 52 μ m respectively. The 85.1% sensitivity and 91.7% specificity in this study for differentiating normal from glaucomatous optic nerves is consistent with the 81% sensitivity at 95% specificity in the Chauhan study.⁶ The results of the current study confirm the stated hypothesis that MRW is significantly thinner in glaucomatous versus non-glaucomatous eyes, and demonstrate the MRW parameter’s utility for glaucoma detection in a population of U.S. Veterans.

GROUP 2 INTER-EYE PAIRED ANALYSIS

MRW was thinner in more advanced vs. less advanced eyes of glaucomatous participants when using global and sectoral analyses, except in the superior-temporal and nasal sectors (though there was a trend towards thinning in superior-temporal sector; $P = .06$). Since glaucoma is known to preferentially affect the inferior temporal rim first and spares the nasal rim until advanced disease states, the low prevalence of advanced disease in this study as defined by VF MD may explain these findings (see Figure 2 above displaying the range of mean deviations in the study participants).

AVERAGE ANTERIOR LAMINA CRIBROSA DEPTH

GROUP 1 VS. GROUP 2 ANALYSES

In the current study, there was a deeper aALCD in glaucomatous vs. non-glaucomatous participants and in test (more severe) vs. fellow (less severe) glaucomatous eyes, but these differences did not meet statistical significance ($P = .17$ and $P = .73$, respectively). This was unexpected since studies have shown statistically significant differences in ALCD between glaucomatous and non-

glaucomatous eyes,²⁷ between pre-perimetric glaucoma vs. normal eyes, and between mild to moderate glaucomatous eyes vs. pre-perimetric eyes.²⁸ Although the power to detect differences in MRW between groups was adequate, due to the simplicity of the novel ALCD measurement method in this study (measuring the depth at only 3 points), the power to detect a difference in these groups for ALCD may not have been adequate. It may also be that the glaucoma population described in this study did not have as significant a pathological change to the optic nerve head structure as previously described populations. A consensus on the best method for describing the deformation of the optic nerve head has not been achieved. Previous studies have used more reference points when measuring the lamina cribrosa depth than the current study.^{27,28} Another study describes measuring the maximum depressed point of 12 b-scans.¹⁷ Additionally, Kim et al. measured the lamina cribrosa curvature with the aid of additional image processing software.²⁹ The simple method described here can be used easily in clinical settings, but further study is required to determine if simplified modifications of the technique are useful for differentiating between glaucomatous and non-glaucomatous optic nerves.

GROUP 2 INTER-EYE PAIRED ANALYSES (POST-HOC)

In post-hoc analysis, the inter-eye aALCD, gMRW, gRNFL, PSD, and BMO area differences were calculated by subtracting the respective values of the fellow eye (less affected) from the test (more affected) eye (Δ aALCD, Δ gMRW, Δ gRNFL, Δ PSD, and Δ BMO area respectively). This post-hoc calculation was of interest as a novel descriptor of the inter-eye variability of the study parameters in glaucoma patients. Figure 4D supports the symmetric nature of the Δ BMO areas between test and fellow eyes. This helps to rule out any question of the BMO having a systematic effect on the other parameters (gMRW or aALCD) reported here. The Δ PSD values (Figure 4C) show the generally mild asymmetry in functional glaucomatous damage between eyes of glaucomatous participants, and are all positive (as expected, given the inclusion criterion).

Next, post-hoc correlations were performed between each of the delta values to further describe their relationships. Moderate negative post-hoc correlations between the Δ gMRW and Δ PSD ($r = -0.46$) and Δ gRNFL and Δ PSD ($r = -0.46$) were found in this study, demonstrating that inter-eye glaucomatous structural asymmetry detected by MRW correlates well with functional visual field asymmetry (i.e., patients with more asymmetry in MRW also show more asymmetry in PSD). Additionally, the relationship is similar to the relationship between RNFL and visual field PSD. In other words, MRW (like RNFL) may be a useful comparative parameter when assessing structural symmetry between the eyes of patients with glaucoma.

This study also found a significant moderately-negative correlation between Δ gMRW and Δ aALCD between test and fellow eyes of glaucoma participants in post-hoc analysis, despite similar BMO areas. This indicates that, independent of optic nerve diameter, when the global minimum rim width is thinner in the glaucomatous eye there is also a significantly larger (deeper) aALCD. The same post-hoc comparison between Δ gRNFL and Δ aALCD was not significant ($P = 0.10$). Along the same line, Fortune et al. hypothesized that MRW was more affected than RNFL by glaucomatous morphological changes in the optic nerve, also finding that the correlation of pRNFLT with the total number of axons in rodent optic nerves was stronger than the correlation of gMRW to the axon count ($r = 0.81$ and $r = 0.72$ respectively).³⁰ If this hypothesis were true, the relationship between Δ gMRW and Δ aALCD found in the present study would also likely be more correlated than Δ gRNFL and Δ aALCD. For instance, if additional bowing of the lamina caused displacement or stretching of the pre-laminar tissue more severely in the test eye than in the fellow eye, this would comparatively thin the MRW, whereas this effect would not be found as strongly for gRNFL. Future longitudinal studies of MRW in humans could help determine the timing and impact of increased ALCD on MRW, and how this may be used clinically for the early detection of glaucoma.

STRENGTHS AND LIMITATIONS

This study was not funded and there were no conflicts of interest for any of the authors. This cross-sectional study validates and moves forward the body of literature describing OCT measures of the optic nerve head in glaucoma, using new MRW and aALCD measurements. The use of inter-eye comparison among the glaucoma subjects is beneficial because glaucoma is generally an asymmetric, bilateral disease and because most studies only describe a single eye of participants with glaucoma. The current study uses the pattern standard deviation to differentiate between the more affected (test) and less affected eyes of glaucoma participants. This differentiation helps to allow for a more intuitive grasp of how these results may apply to a patient in the clinical setting.

The relatively small number of participants and lack of diversity are limitations. The study was also not designed with consideration of glaucoma severity, and indeed, a majority of participants had mild glaucoma based on the average visual field MD; thus the findings cannot be generalized to more advanced levels of glaucoma. While no participant with glaucoma demonstrated signs of progressive disease up to the point of recruitment, 55% of glaucomatous subjects had fields taken on a different day than other test data. Since the average time between OCT

data and visual field was 3 months, we cannot rule-out the possibility that disease progression occurred in that time interval. Additionally, since the eye in non-glaucomatous participants with better visual acuity or lower refractive error (per the inclusion criterion) was selected, this could introduce a selection bias, though it is reassuring that spherical equivalent was not statistically different between groups and visual acuity was at least 20/40 in all cases. The interesting findings surrounding $\Delta gMRW$ and $\Delta aALCD$ in this study should be interpreted cautiously, since these were demonstrated in post-hoc analysis. Finally, this study did not measure the reproducibility of the ALCD measurement, which would be required for validation before future use.

CONCLUSION

The new optical coherence tomography parameter “Bruch’s membrane opening-minimum rim width” (MRW) differentiates between glaucomatous vs. non-glaucomatous optic nerves in this Veteran population (85% sensitivity, 92% specificity). Anterior lamina cribrosa depth can be easily measured in clinic using the same scanning protocols required for MRW. In the current study, lamina were non-significantly deeper in glaucomatous vs. non-glaucomatous participants, and were also non-significantly deeper in glaucomatous eyes with more affected visual fields vs. fellow eyes. In the groups of more-affected and less affected eyes of glaucomatous participants in this study, there was a statistically thinner gMRW, and 4 of the 6 specific MRW sectors were also statistically thinner. Post-hoc inter-eye data analysis of glaucomatous eyes suggested that MRW measurements can detect the asymmetry of glaucoma in an individual, and that inter-eye differences in MRW values reflect well the asymmetric damage in glaucoma as correlated with the visual field.

Additional studies are required which characterize the morphology of the optic nerve head in various stages of glaucoma and over time as glaucoma develops. Such studies may lead to clinically-useful and easy-to-perform tests, with the goal of earlier disease detection.

REFERENCES

1. Yang H, Reynaud J, Lockwood H, et al. The connective tissue phenotype of glaucomatous cupping in the monkey eye - clinical and research implications. *Prog Retin Eye Res.* 2017;59:1-52.
doi: [10.1016/j.preteyeres.2017.03.001](https://doi.org/10.1016/j.preteyeres.2017.03.001)

2. Quigley HA, Addicks EM. Chronic experimental glaucoma in primates. II. Effect of extended intraocular pressure elevation on optic nerve head and axonal transport. *Invest Ophthalmol Vis Sci.* 1980;19(2):137-152.
3. Sigal IA, Flanagan JG, Ethier CR. Factors influencing optic nerve head biomechanics. *Invest Ophthalmol Vis Sci.* 2005;46(11):4189-4199. doi: [10.1167/iovs.05-0541](https://doi.org/10.1167/iovs.05-0541)
4. Luo H, Yang H, Gardiner SK, et al. Factors influencing central lamina cribrosa depth: a multicenter study. *Invest Ophthalmol Vis Sci.* 2018;59(6):2357-2370. doi: [10.1167/iovs.17-23456](https://doi.org/10.1167/iovs.17-23456)
5. Reis AS, Sharpe GP, Yang H, Nicoleta MT, Burgoyne CF, Chauhan BC. Optic disc margin anatomy in patients with glaucoma and normal controls with spectral domain optical coherence tomography. *Ophthalmology.* 2012;119(4):738-747. doi: [10.1016/j.ophtha.2011.09.054](https://doi.org/10.1016/j.ophtha.2011.09.054)
6. Chauhan BC, O'Leary N, Almobarak FA, et al. Enhanced detection of open-angle glaucoma with an anatomically accurate optical coherence tomography-derived neuroretinal rim parameter. *Ophthalmology.* 2013;120(3):535-543. doi: [10.1016/j.ophtha.2012.09.055](https://doi.org/10.1016/j.ophtha.2012.09.055)
7. Reis ASC, O'Leary N, Yang H, et al. Influence of clinically invisible, but optical coherence tomography detected, optic disc margin anatomy on neuroretinal rim evaluation. *Invest Ophthalmol Vis Sci.* 2012;53(4):1852-1860. doi: [10.1167/iovs.11-9309](https://doi.org/10.1167/iovs.11-9309)
8. Reis AC, Zangalli C, Abe R, et al. Intra- and interobserver reproducibility of Bruch's membrane opening minimum rim width measurements with spectral domain optical coherence tomography. *Acta Ophthalmol.* 2017;95(7):e548-e555. doi: [10.1111/aos.13464](https://doi.org/10.1111/aos.13464)
9. Park K, Kim J, Lee J. Reproducibility of Bruch's membrane opening-minimum rim width measurements with spectral domain optical coherence tomography. *J Glaucoma.* 2017;26(11):1041-1050. doi: [10.1097/IJG.0000000000000787](https://doi.org/10.1097/IJG.0000000000000787)
10. Heidelberg Engineering. *Spectralis HRA+OCT User Manual (Software Version 6.6)*. Heidelberg Engineering; 2016.
11. Burgoyne CF, Crawford Downs J, Bellezza AJ, Francis Suh JK, Hart RT. The optic nerve head as a biomechanical structure: a new paradigm for understanding the role of IOP-related stress and strain in the pathophysiology of glaucomatous optic nerve head damage. *Prog Retin Eye Res.* 2005;24(1):39-73. doi: [10.1016/j.preteyeres.2004.06.001](https://doi.org/10.1016/j.preteyeres.2004.06.001)
12. Gmeiner JMD, Schrems WA, Mardin CY, Laemmer R, Kruse FE, Schrems-Hoesl LM. Comparison of Bruch's membrane opening minimum rim width and peripapillary retinal nerve fiber layer thickness in early glaucoma assessment. *Invest Ophthalmol Vis Sci.* 2016;57(9):OCT575-OCT584. doi: [10.1167/iovs.15-18906](https://doi.org/10.1167/iovs.15-18906)

13. He L, Yang H, Gardiner SK, et al. Longitudinal detection of optic nerve head changes by spectral domain optical coherence tomography in early experimental glaucoma. *Invest Ophthalmol Vis Sci*. 2014;55(1):574-586. doi: [10.1167/iovs.13-13245](https://doi.org/10.1167/iovs.13-13245)
14. Levy NS, Crapps EE. Displacement of optic nerve head in response to short-term intraocular pressure elevation in human eyes. *Arch Ophthalmol*. 1984;102(5):782-786. doi: [10.1001/archophth.1984.01040030630037](https://doi.org/10.1001/archophth.1984.01040030630037)
15. Bellezza AJ, Rintalan CJ, Thompson HW, Downs JC, Hart RT, Burgoyne CF. Deformation of the lamina cribrosa and anterior scleral canal wall in early experimental glaucoma. *Invest Ophthalmol Vis Sci*. 2003;44(2):623-637. doi: [10.1167/iovs.01-1282](https://doi.org/10.1167/iovs.01-1282)
16. Yang H, Downs JC, Bellezza A, Thompson H, Burgoyne CF. 3-D histomorphometry of the normal and early glaucomatous monkey optic nerve head: prelaminar neural tissues and cupping. *Invest Ophthalmol Vis Sci*. 2007;48(11):5068-5084. doi: [10.1167/iovs.07-0790](https://doi.org/10.1167/iovs.07-0790)
17. Lanzagorta-Aresti A, Perez-Lopez M, Palacios-Pozo E, Davo-Cabrera J. Relationship between corneal hysteresis and lamina cribrosa displacement after medical reduction of intraocular pressure. *Br J Ophthalmol*. 2016;101(3):290-294. doi: [10.1136/bjophthalmol-2015-307428](https://doi.org/10.1136/bjophthalmol-2015-307428)
18. Lee EJ, Kim TW, Weinreb RN. Reversal of lamina cribrosa displacement and thickness after trabeculectomy in glaucoma. *Ophthalmology*. 2012;119(7):1359-1366. doi: [10.1016/j.ophtha.2012.01.034](https://doi.org/10.1016/j.ophtha.2012.01.034)
19. Lee SH, Yu DA, Kim TW, Lee EJ, Girard MJA, Mari JM. Reduction of the lamina cribrosa curvature after trabeculectomy in glaucoma. *Invest Ophthalmol Vis Sci*. 2016;57(11):5006-5014. doi: [10.1167/iovs.15-18982](https://doi.org/10.1167/iovs.15-18982)
20. Reis ASC, O'Leary N, Stanfield MJ, Shuba LM, Nicolela MT, Chauhan BC. Lamina displacement and prelaminar tissue thickness change after glaucoma surgery imaged with optical coherence tomography. *Invest Ophthalmol Vis Sci*. 2012;53(9):5819-5826. doi: [10.1167/iovs.12-9924](https://doi.org/10.1167/iovs.12-9924)
21. Yoshikawa M, Akagi T, Hangai M, et al. Alterations in the neural and connective tissue components of glaucomatous cupping after glaucoma surgery using swept-source optical coherence tomography. *Invest Ophthalmol Vis Sci*. 2014;55(1):477-484. doi: [10.1167/iovs.13-11897](https://doi.org/10.1167/iovs.13-11897)
22. Lee EJ, Kim TW. Lamina cribrosa reversal after trabeculectomy and the rate of progressive retinal nerve fiber layer thinning. *Ophthalmology*. 2015;122(11):2234-2242. doi: [10.1016/j.ophtha.2015.07.020](https://doi.org/10.1016/j.ophtha.2015.07.020)
23. Bellezza AJ, Hart RT, Burgoyne CF. The optic nerve head as a biomechanical structure: initial finite element modeling. *Invest Ophthalmol Vis Sci*. 2000;41(10):2991-3000.

24. Rhodes LA, Huisingh C, Johnstone J, et al. Variation of lamina depth in normal eyes with age and race. *Invest Ophthalmol Vis Sci.* 2014;55(12):8123-8133. doi: [10.1167/iovs.14-1525](https://doi.org/10.1167/iovs.14-1525)
25. Wilkinson CP, Ferris FL, Klein RE, et al. Proposed international clinical diabetic retinopathy and diabetic macular edema disease severity scales. *Ophthalmology.* 2003;110(9):1677-1682. doi: [10.1016/S0161-6420\(03\)00475-5](https://doi.org/10.1016/S0161-6420(03)00475-5)
26. Age-Related Eye Disease Study Research Group. A randomized, placebo-controlled, clinical trial of high-dose supplementation with vitamins C and E, beta carotene, and zinc for age-related macular degeneration and vision loss: AREDS report no. 8. *Arch Ophthalmol.* 2001;119(10):1417-1436. doi: [10.1001/archophth.119.10.1417](https://doi.org/10.1001/archophth.119.10.1417)
27. Furlanetto RL, Park SC, Damle UJ, et al. Posterior displacement of the lamina cribrosa in glaucoma: in vivo interindividual and intereye comparisons. *Invest Ophthalmol Vis Sci.* 2013;54(7):4836-4842. doi: [10.1167/iovs.12-11530](https://doi.org/10.1167/iovs.12-11530)
28. Park SC, Brumm J, Furlanetto RL, et al. Lamina cribrosa depth in different stages of glaucoma. *Invest Ophthalmol Vis Sci.* 2015;56(3):2059-2064. doi: [10.1167/iovs.14-15540](https://doi.org/10.1167/iovs.14-15540)
29. Kim J-A, Kim T-W, Lee EJ, Girard MJA, Mari JM. Comparison of lamina cribrosa morphology in eyes with ocular hypertension and normal-tension glaucoma. *Invest Ophthalmol Vis Sci.* 2020;61(4):4-4. doi: [10.1167/iovs.61.4.4](https://doi.org/10.1167/iovs.61.4.4)
30. Fortune B, Hardin C, Reynaud J, et al. Comparing optic nerve head rim width, rim area, and peripapillary retinal nerve fiber layer thickness to axon count in experimental glaucoma. *Invest Ophthalmol Vis Sci.* 2016;57(9):OCT404-OCT412. doi: [10.1167/iovs.15-18667](https://doi.org/10.1167/iovs.15-18667)